Hindawi Publishing Corporation
International Journal of Optics
Volume 2011, Article ID 374581, 6 pages
doi:10.1155/2011/374581

Research Article

Nonlinear Phenomena of Ultra-Wide-Band Radiation in a Photonic Crystal Fibre

Rim Cherif and Mourad Zghal

Cirta'Com laboratory, Engineering School of Communication of Tunis (Sup'Com), University of Carthage, Ghazala Technopark, Ariana 2083, Tunisia

Correspondence should be addressed to Rim Cherif, rim.cherif@supcom.rnu.tn

Received 22 May 2011; Revised 2 September 2011; Accepted 7 September 2011

Academic Editor: Wojtek J. Bock

We report the results of a numerical and experimental analysis of femtosecond pulse propagation in a highly nonlinear photonic crystal fibre (PCF). The propagation of ultrashort pulses in PCF is studied taking into account the effects of dispersion, self-phase modulation, stimulated Raman scattering, and self-steepening. The interaction between linear and nonlinear effects is investigated in order to better understand the interplay of these effects leading to the supercontinuum generation. The initial stage of an ultra-wide-band supercontinuum generation under femtosecond pumping is pointed out. Details about the expansion of the blue and red sides of the supercontinuum due to transfer of energy to dispersive waves are revealed and experimentally confirmed. Our experimental results are compared to numerical solution of the nonlinear Schrödinger equation. Good agreement is found.

1. Introduction

The generation of new frequency components also referred to as supercontinuum generation (SCG) obtained by focusing intense light in a nonlinear medium has been well known since the 1970's [1]. The emergence of photonic crystal fibres (PCFs) in the late 1990s has attracted widespread interest throughout the scientific community and has led to the revolution in the SCG [2, 3]. PCFs consist of a solid core surrounded by an ordered array of microscopic air holes running along the fibre length [4, 5]. These fibres have revealed unusual properties that cannot be offered by conventional fibres. Photonic crystal fibre with a small core can cause the zero dispersion wavelength (ZDW) to be shifted to wavelength significantly shorter than the ZDW of standard single-mode silica fibres [6, 7]. At the same time, the relatively low nonlinearity of silica is offset by the small effective area of PCF that gives a very high nonlinear response for low pump power [8]. These particular properties have made PCF an ideal candidate for compact and cost-effective telecommunication devices with short fibres and relatively low-cost light sources, which are the principal drawbacks of previously demonstrated fibre-based nonlinear optical devices [9–12]. The white-light source has found numerous applications in diverse fields such as spectroscopy, pulse compression, and design of tunable ultrafast femtosecond laser sources. In telecommunications, the spectral slicing of broadband SC spectra has been proposed as a simple technique to create multiwavelength optical sources for dense wavelength division multiplexing application [13]. The growing interest to this phenomenon has led to a steady progress in the understanding of the interplay between the different nonlinear processes affecting high-power radiation evolution in the optical fibre waveguide. The complex mechanisms behind the extremely wide spectra obtained have been investigated both numerically and experimentally by several groups. Among the different nonlinear processes, the generation of dispersive waves has received considerable attention [14–17].

In this paper, we present an experimental and numerical analysis of femtosecond pulse propagation in a highly nonlinear multimode PCF. Most of the works published in this area reported the SC generated by the fundamental mode. In our previous paper, we presented experimental results of SC generated by high-order modes [18]. In this

contribution, we present a review paper containing a complete and exhaustive numerical and experimental analysis of SCG in a highly nonlinear multimode PCF. We experimentally investigate the initial stage of an ultra-wide-band supercontinuum generation in a PCF under femtosecond pumping in normal and anomalous dispersion regime. We show that when the pump wavelength is close to the zero-dispersion wavelength, a wide and uniform spectral broadening is achieved. Details about the expansion of the blue and red sides of the supercontinuum due to the transfer of energy to dispersive waves are revealed and experimentally confirmed. The dispersion profile has profound influence on the nonlinear processes taking place in the fibre. We present a detailed analysis of the phenomenon through numerical simulations which take into account the effects of high-order dispersion, self-phase modulation (SPM), stimulated Raman scattering (SRS), and self-steepening (SS).

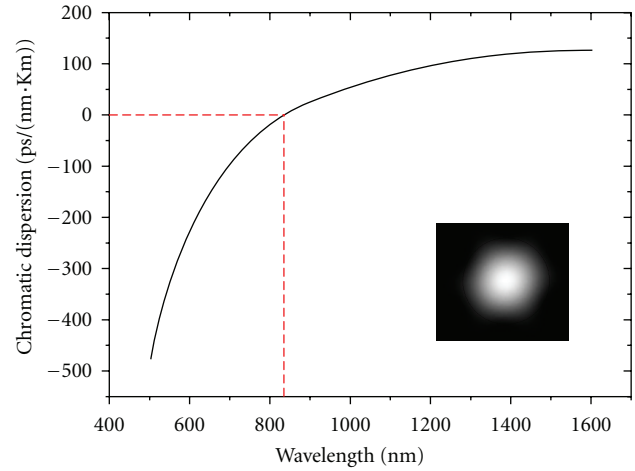

Figure 1: Computed chromatic dispersion of the fundamental mode versus wavelength.

2. Ultrashort Pulse Propagation Modelling

Pulse propagation in PCF is well described by the generalized nonlinear Schrödinger equation (GNLSE) [19]. It includes the linear effects of attenuation and dispersion, Kerr and stimulated Raman scattering as nonlinear effects scaling with the nonlinearity parameter. It describes the temporal and longitudinal dependency of the slowly varying pulse envelope $U(z,t)$ in a frame of reference moving at the group velocity of the pulse, $v_g = 1/\beta_1$

$$\frac{\partial U}{\partial z} = -\frac{\alpha}{2}U - \sum_{m\geq 2}\frac{j^{m-1}\beta_m}{m!}\frac{\partial^m U}{\partial t^m} + j\gamma\left(1+\frac{j}{\omega_0}\frac{\partial}{\partial t}\right), \times\left(U(z,t)\int_{-\infty}^{+\infty}R(t')\left|U(z,t-t')\right|^2 dt'\right). \quad (1)$$

In the above equation, U is the pulse envelope variation, α is the attenuation constant, β_m are the various coefficients in the Taylor series expansion of propagation constant β at the input pulse's central frequency ω_0, and γ is the nonlinear coefficient. The time derivative on the right-hand side of (1) includes the effects of SS and SRS. The response function $R(t)$ includes the electronic and the vibrational Raman contributions

$$R(t) = (1-f_r)\delta(t) + f_r h_r(t), \quad (2)$$

where $f_r = 0.18$ and $h_r(t)$ is the Raman response function of the silica core

$$h_r(t) = \frac{\tau_1^2+\tau_2^2}{\tau_1\tau_2^2}\exp\left(\frac{-t}{\tau_2}\right)\sin\left(\frac{t}{\tau_1}\right) \quad (3)$$

with $\tau_1 = 12.2$ fs and $\tau_2 = 32$ fs [19].

In our investigation, (1) has been solved numerically using the symmetrized split-step Fourier method [19]. This method is attractive because of its accuracy and time speed calculations. The fundamental assumption of this method consists of solving (1) for steps dz small enough that the dispersive (linear) step and the nonlinear one can be taken separately. Linear and nonlinear steps are calculated in the frequency and time domain space, respectively. The numerical integration of the nonlinear part is performed using a fourth order Runge-Kutta method. In our simulations, the temporal resolution is equal to 4 fs. The number of time samples is 2×10^{13}. The spatial step dz was chosen around 50 μm.

3. Results and Discussions

The air-silica microstructured photonic crystal fibre used in our study is made up of holes with a 2.5-μm average diameter which are arranged in a hexagonal pattern with a 2.7-μm pitch. The linear dimension of the solid core is about 2.2 μm. The fibre has a nonlinear coefficient $\gamma = 72\,(\mathrm{W}\cdot\mathrm{Km})^{-1}$ at 850 nm. Using the real cross-section of the PCF, the chromatic dispersion has been computed for a wavelength range extending from 500 nm to 1600 nm. The calculations were performed by using full vectorial modal solver based on finite element method, where the material dispersion given by Sellmeier's formula is directly included in the calculations [20]. The assumed dispersion characteristic of the PCF is shown in Figure 1. The fibre exhibits a zero-dispersion wavelength around 840 nm. It is characterized by a very small core diameter that enhances its nonlinear properties. This PCF with nearly zero dispersion slope and small effective mode area would be useful for broadband SC generation, soliton pulse transmission, nonlinear optical loop mirror, and wavelength conversion.

3.1. Nonlinear Propagation in a PCF. In order to better understand the construction of SC, a detailed analysis of femtosecond pulse propagation is presented. In our simulations, the pulse has a width of 100 fs and has a hyperbolic secant field profile. The repetition rate of the pulse is 80 MHz. The laser average power is equal to 300 mW. Figure 2 shows the pulse evolution when only second-order dispersion is considered. We notice that the pulse broadens under the effect of second-order dispersion (SOD). In fact, SOD

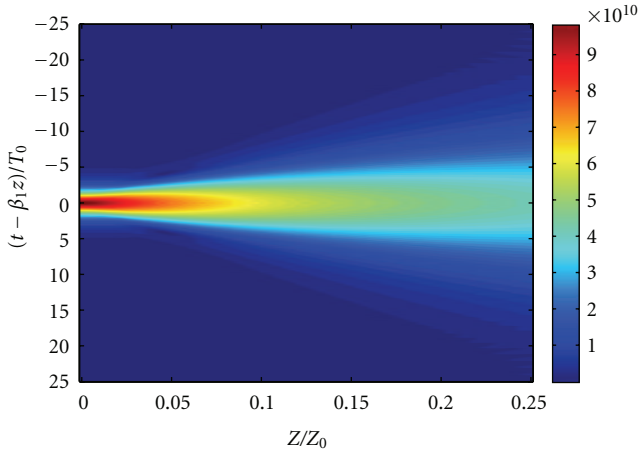

Figure 2: Temporal evolution at propagation distance of 25-cm for pump wavelength $\lambda = 850$ nm. Only dispersion is taken into account.

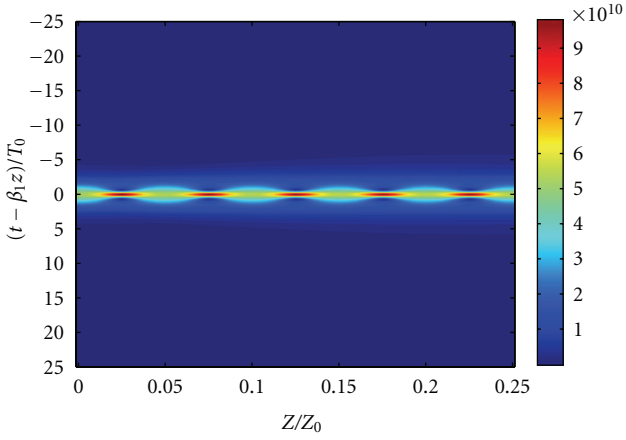

Figure 3: Temporal evolution at propagation distance of 25-cm for pump wavelength $\lambda = 850$ nm. Kerr nonlinearity and dispersion are taken into account.

changes the phase of each spectral component of the pulse by an amount that depends on the frequency and the propagated distance. Short pulses broaden more rapidly because of their smaller dispersion length.

Figure 3 depicts soliton propagation in the anomalous dispersion regime. The soliton is an exact solution of the GNLSE with Kerr nonlinearity (responsible for the SPM effect) and negative second-order dispersion β_2 as given in (1). The soliton appears because the dispersion broadening in the fibre is compensated by the intensity-dependant SPM. After a soliton period, the pulse reverts to its initial state. We clearly see that the pulse velocity is equal to the group velocity of the soliton which consequently stays centred at $t = 0$ s.

The Raman perturbation of periodic soliton evolution is shown in the numerical results of Figure 4. The velocity is slightly different from the group velocity of the pulse, which makes the centre of the pulse shift to positive time values. Apart from this shift of the centre, due to the velocity offset,

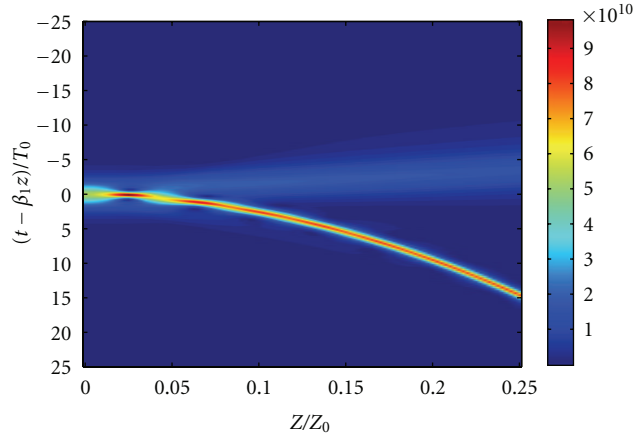

Figure 4: Temporal evolution at propagation distance of 25-cm for pump wavelength $\lambda = 850$ nm. Kerr nonlinearity, dispersion, and SRS are taken into account.

the behaviour of the pulses in Figures 3 and 4 is equivalent and is described as the evolution of a higher-order soliton.

3.2. Supercontinuum Generation. Based on the above results, we experimentally and numerically analyze the interplay of linear and nonlinear effects in order to understand the construction of the SCG. The experimental setup is depicted in Figure 5. The light source is a cw-mode locked Ti : Sapphire laser delivering a train of 100 fs pulses at the repetition rate of 80 MHz. The maximum average power coupled into the fibre is around 300 mW. The wavelength can be tuned from 700 nm to 900 nm. In order to avoid harmful back reflections from the input tip of the fibre we employ a Faraday isolator. The laser beam is coupled into a PCF span of 25-cm length by means of an aspheric lens having a numerical aperture of 0.65. The fibre is mounted on a three-axis translation stage allowing the positioning of the fibre with a resolution of 20 nm. The spectral properties of the output radiation are monitored by an optical spectrum analyser having a resolution of 0.1 nm.

In our experiment, we used $\lambda = 850$ nm as a pump wavelength. SC generation in the 850 nm region has important applications such as spectral-slicing pulse source, optical wavelength converter, and all-optical signal processing. Note that the considered input wavelength is in the anomalous region, and, therefore, soliton dynamics plays a crucial role in the propagation. Many studies reported the dynamics of the supercontinuum generation which is dominated by fission of solitons which emit phase-matched dispersive waves in a typical PCF with one ZDW [21, 22].

Figure 6 shows the numerical spectrum obtained with the same experimental parameters. To model the dispersion characteristics of our PCF, we considered the Taylor expansion up to the 10th order. By taking $\lambda = 850$ nm as the central wavelength of the input pulse, the calculated dispersion coefficient values of the expansion are $\beta_2 = -9.0026\,\text{ps}^2/\text{km}$, $\beta_3 = 0.068295\,\text{ps}^3/\text{km}$, $\beta_4 = -0.10229\text{e}^{-3}\,\text{ps}^4/\text{km}$, $\beta_5 = 2.0338\text{e}^{-7}\,\text{ps}^5/\text{km}$, $\beta_6 = -1.3695\text{e}^{-10}\,\text{ps}^6/\text{km}$,

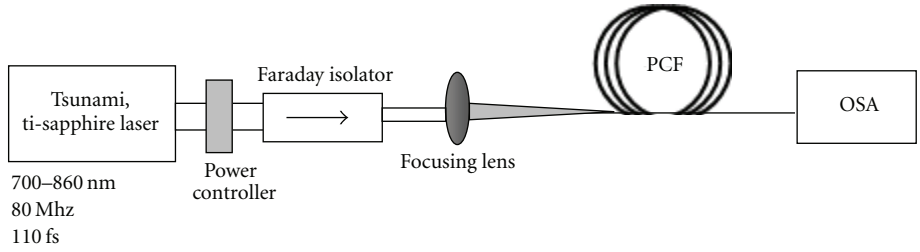

Figure 5: Experimental setup for supercontinuum generation.

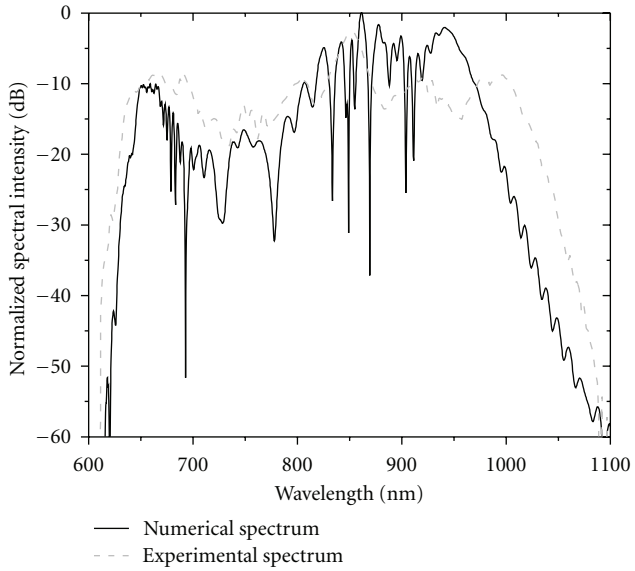

Figure 6: Comparison between numerical and experimental spectrum of supercontinuum generation.

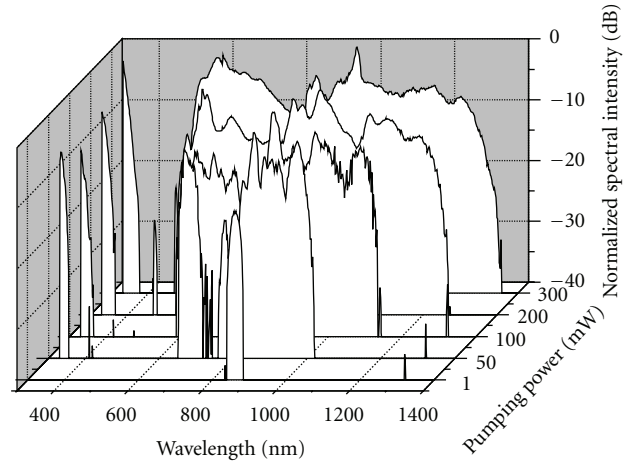

Figure 7: Experimental spectra for a 25-cm-long PCF versus wavelength at 850 nm.

$\beta_7 = -3.0396e^{-10}$ ps^7/km, $\beta_8 = -1.7507e^{-14}$ ps^8/km, $\beta_9 = 1.3343e^{-16}$ ps^9/km, and $\beta_{10} = -5.3943e^{-19}$ ps^{10}/km. Good agreement was found between experimental and numerical results.

Figure 7 shows a set of recorded spectra obtained by increasing progressively the input power P. For low input power, distinct spectral peaks are observed. The spectral broadening is mainly due to SPM and asymmetry induced by the Raman scattering effect, and also the high dispersion slope is depicted. At 50 mW, the peak around 920 nm is the first soliton formed and subsequently self-frequency shifted to longer wavelengths as the pumping power is increased.

At this stage, let us recall that the soliton number is defined as $N^2 = \gamma P_0 L_D$, where P_0 is the peak power, L_D is the dispersion length, and γ is the nonlinear coefficient of the fibre. The fundamental soliton splits into N higher-order soliton pulses with different red-shifted central frequencies and different group velocities. After the fission every pulse emits a dispersive wave phase matched to the corresponding pulse which is simultaneously moving to the infra red region. Increasing the pump power further leads to a merging of the various spectral components and to a subsequent formation of a supercontinuum that extends from 350 nm to beyond 1370 nm. Besides, the phase of the soliton at frequency ω_p should overlap with that of the dispersive wave at frequency ω_d. If we call $\beta(\omega)$ the frequency-dependent wave vector of the optical signal, a phase matching condition is expressed as [19]

$$\Delta\kappa = \frac{\beta(\omega) - \beta\left(\omega_p\right) - \left(\omega - \omega_p\right)}{u_g - \gamma P_0} = 0, \tag{4}$$

where u_g is the group velocity at frequency ω_p, γ is the fibre nonlinear coefficient, and P_0 is the soliton peak power. The dispersive wave having a low spectral density is supposed to propagate in the linear regime. We predict for the dispersive radiation a wavelength of 670 nm. Good agreement between numerical and experimental results is found.

When pumping in the normal dispersion regime, at $\lambda = 805$ nm, we obtain the set of spectra shown in Figure 8.

We notice from Figure 8 that the spectral broadening is also ruled by the effects of soliton self-frequency shift and the induced dispersive wave. Thus, the obtained SC is extending from 350 nm to 1100 nm. The blue part of the spectrum is attributed to the generation of the Cerenkov radiation.

When pumping at wavelengths around 800 nm, we start observing the different high-order modes, so that we fulfilled the selective excitation of one specific mode, as such study was not investigated in the literature. We report in Figure 9

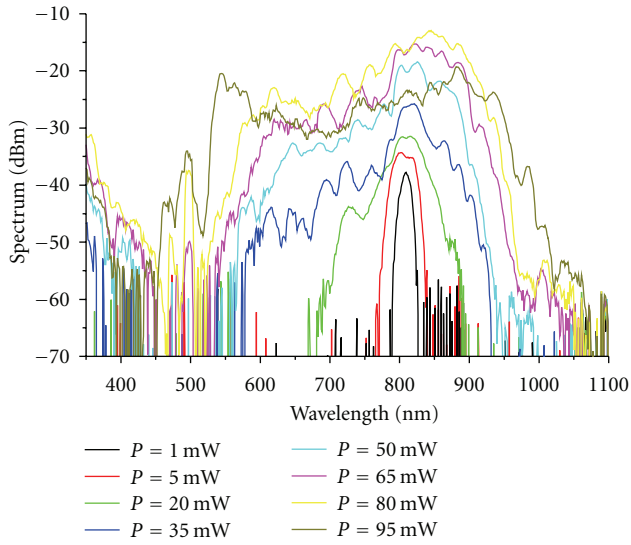

Figure 8: Experimental spectra for a 25-cm-long PCF versus wavelength at 805 nm.

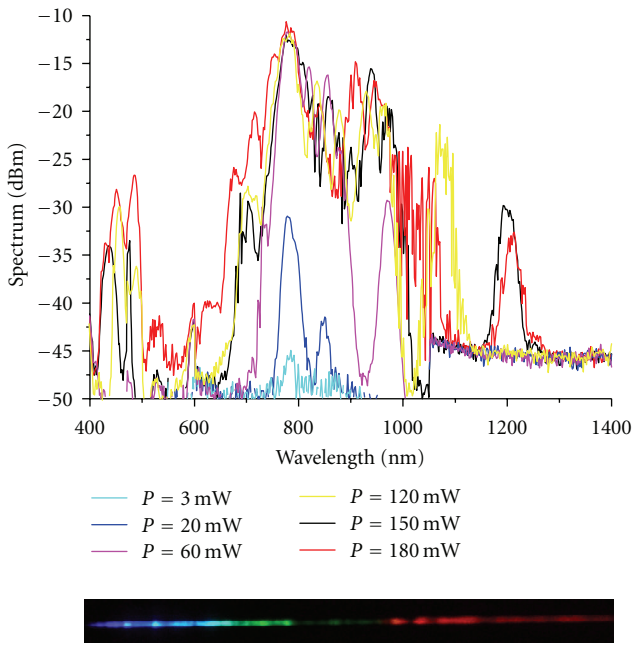

Figure 9: Experimental spectra for a 25-cm-long PCF versus wavelength at 785 nm. The SC is generated by the first high-order mode LP11.

the set of spectra recorded for the first high-order mode when pumping at the optimized $\lambda = 785$ nm.

As seen from Figure 9, the SC generated by the first high-order mode is extending from 400 nm to more than 1200 nm. The mechanisms behind the SCG are investigated showing that the Raman effect is responsible for the soliton generation at 830 nm and then frequency shifted inducing the dispersive wave generation towards visible wavelengths range.

4. Conclusion

As a conclusion, we have presented numerical and experimental results describing the nonlinear propagation of femtosecond pulses in a photonic crystal fibre. The mechanism behind the spectral broadening is mainly ruled by soliton propagation leading to the generation of a blue-shifted dispersive wave. Our experimental results are compared to numerical ones obtained by means of a numerical solution of the nonlinear Schrödinger equation. Good agreement between experimental and numerical results was found. We have demonstrated a smooth, broad, and powerful SC light source centred around 850 nm. Supercontinuum generation in nonlinear photonic crystal fibres is highly influenced by the choice of pumping wavelength as both the zero-dispersion wavelength and the absolute dispersion at the pumping wavelength has a profound impact on the nonlinear processes. The SC generated by high-order mode was discussed. Broadband spectra were observed when selecting the LP11 mode.

References

[1] R. R. Alfano and S. L. Shapiro, "Emission in the region 4000 to 7000 A via four-photon coupling in glass," *Physical Review Letters*, vol. 24, no. 11, pp. 584–587, 1970.

[2] J. K. Ranka, R. S. Windeler, and A. J. Stentz, "Visible continuum generation in air-silica microstructure optical fibers with anomalous dispersion at 800 nm," *Optics Letters*, vol. 25, no. 1, pp. 25–27, 2000.

[3] S. Coen, A. H. L. Chau, R. Leonhardt et al., "White-light supercontinuum generation with 60 ps pump pulses in a photonic crystal fiber," *Optics Letters*, vol. 26, no. 17, pp. 1356–1358, 2001.

[4] T. M. Monro and D. J. Richardson, "Holey optical fibres: fundamental properties and device applications," *Comptes Rendus Physique*, vol. 4, no. 1, pp. 175–186, 2003.

[5] P. S. J. Russell, "Photonic-crystal fibers," *Journal of Lightwave Technology*, vol. 24, no. 12, pp. 4729–4749, 2006.

[6] J. Broeng, D. Mogilevstev, S. E. Barkou, and A. Bjarklev, "Photonic crystal fibers: a new class of optical waveguides," *Optical Fiber Technology*, vol. 5, no. 3, pp. 305–330, 1999.

[7] J. C. Knight, J. Arriaga, T. A. Birks, A. Ortigosa-Blanch, W. J. Wadsworth, and P. S. J. Russell, "Anomalous dispersion in photonic crystal fiber," *IEEE Photonics Technology Letters*, vol. 12, no. 7, pp. 807–809, 2000.

[8] N. G. R. Broderick, T. M. Monro, P. J. Bennett, and D. J. Richardson, "Nonlinearity in holey optical fibers: measurement and future opportunities," *Optics Letters*, vol. 24, no. 20, pp. 1395–1397, 1999.

[9] A. V. Husakou and J. Herrmann, "Supercontinuum generation of higher-order solitons by fission in photonic crystal fibers," *Physical Review Letters*, vol. 87, no. 20, Article ID 203901, pp. 203901/1–203901/4, 2001.

[10] G. Genty, M. Lehtonen, H. Ludvigsen, J. Broeng, and M. Kaivola, "Spectral broadening of femtosecond pulses into continuum radiation in microstructured fibers," *Optics Express*, vol. 10, no. 20, pp. 1083–1098, 2002.

[11] M. Lehtonen, G. Genty, H. Ludvigsen, and M. Kaivola, "Supercontinuum generation in a highly birefringent microstructured fiber," *Applied Physics Letters*, vol. 82, no. 14, pp. 2197–2199, 2003.

[12] P. A. Champert, V. Couderc, P. Leproux et al., "White-light supercontinuum generation in normally dispersive optical fiber using original multi-wavelength pumping system," *Optics Express*, vol. 12, no. 19, pp. 4366–4371, 2004.

[13] X. Sang, P. L. Chu, and C. Yu, "Applications of nonlinear effects in highly nonlinear photonic crystal fiber to optical communications," *Optical and Quantum Electronics*, vol. 37, no. 10, pp. 965–994, 2005.

[14] R. Cherif, A. B. Salem, M. Zghal et al., "Highly nonlinear As_2Se_3-based chalcogenide photonic crystal fiber for midinfrared supercontinuum generation," *Optical Engineering*, vol. 49, pp. 095002-1–095002-6, 2010.

[15] J. C. Travers, S. V. Popov, and J. R. Taylor, "Extended blue supercontinuum generation in cascaded holey fibers," *Optics Letters*, vol. 30, no. 23, pp. 3132–3134, 2005.

[16] R. Cherif, M. Zghal, I. Nikolov, and M. Danailov, "High energy femtosecond supercontinuum light generation in large mode area photonic crystal fiber," *Optics Communications*, vol. 283, no. 21, pp. 4378–4382, 2010.

[17] L. Tartara, I. Cristiani, and V. Degiorgio, "Blue light and infrared continuum generation by soliton fission in a microstructured fiber," *Applied Physics B: Lasers and Optics*, vol. 77, no. 2-3, pp. 307–311, 2003.

[18] R. Cherif, M. Zghal, L. Tartara, and V. Degiorgio, "Supercontinuum generation by higher-order mode excitation in a photonic crystal fiber," *Optics Express*, vol. 16, no. 3, pp. 2147–2152, 2008.

[19] G. P. Agrawal, *Nonlinear Fibre Optics*, Academic Press, San Diego, Calif, USA, 3rd edition, 1995.

[20] M. Zghal and R. Cherif, "Impact of small geometrical imperfections on chromatic dispersion and birefringence in photonic crystal fibers," *Optical Engineering* vol. 46, no. 12, Article ID 128002, pp. 1–7, 2007.

[21] G. Genty, M. Lehtonen, and H. Ludvigsen, "Route to broadband blue-light generation in microstructured fibers," *Optics Letters*, vol. 30, no. 7, pp. 756–758, 2005.

[22] I. Cristiani, R. Tediosi, L. Tartara, and V. Degiorgio, "Dispersive wave generation by solitons in microstructured optical fibers," *Optics Express*, vol. 12, no. 1, pp. 124–135, 2004.